Optoelectronics Properties Tunability by Controlled Deformation

2016 J. Phys.: Conf. Ser. 707 012010

(http://iopscience.iop.org/1742-6596/707/1/012010)

Optoelectronics Properties Tunability by Controlled Deformation

F.H. Alharbi[1,2], P. Serra[1,3], M.A. Carignano[1], and S. Kais[1,2,4]

[1] Qatar Environment & Energy Research Institute, Qatar Foundation, Doha, Qatar
[2] College of Science & Eningeering (QEERI), Hamad Bin Khalifah University, Doha, Qatar
[3] Facultad de Matemática, Astronomía y Física, Universidad Nacional de Córdoba and IFEG-CONICET, Ciudad Universitaria, X5016LAE Córdoba, Argentina.
[4] Department of Chemistry, Physics, and Birck Nanotechnology Center, Purdue University, West Lafayette, Indiana 47907, USA.

E-mail: falharbi@qf.org.qa

Abstract. Manipulating energy levels while controlling the electron localization is an essential step for many applications of confined systems. In this paper we demonstrate how to achieve electron localization and induce energy level oscillation in one-dimensional quantum systems by externally controlling the deformation of the system. From a practical point of view, the one-dimensional potentials can be realized using layered structures. In the analysis, we considered three different examples. The first one is a graded quantum well between confining infinite walls where the deformation is modeled by varying slightly the graded well. The second systems is a symmetric multiple quantum well between infinite walls under the effect of biasing voltage. The third system is a layered 2D hybrid perovskites where pressure is used to induce deformation. The calculations are conducted both numerically and analytically using the perturbation theory. It is shown that the obtained oscillations are associated with level avoided crossings and that the deformation results in changing the spatial localization of the electrons.

1. Introduction

Over the past decade, manipulating electrons in quantum-confined system has progressed remarkably [1, 2] and thus allows developing devices for many applications like quantum computing [3, 4], spectroscopy [5, 6], ultra-fast and sensitive optoelectronics [7, 8], optical tunability [9, 10], and negative heat capacity [11]. In such devices, it is essential to have well controlled manipulation means. Different manipulation mechanisms are used currently such as superconductor circuits [12, 13] and spins in solids [14] and molecules [15–17]. However, the controllability of confined quantum systems in general and in particular for selected energy levels is still a major challenge [18, 19] that has stimulating the exploration of many new concepts [20–24]. One of the largely investigated control techniques relies on the utilization of Stückelberg oscillations. By passing an avoided crossing twice, the interference due to the dynamical phase between transitions can be either constructive or destructive. This is known as Landau-Zener-Stückelberg (LZS) interference [13, 21, 25]. Usually, the levels' oscillation occurs in the time domain. However, Nori and co-workers showed that this is achievable as well in the space domain using spatially inhomogeneous magnetic field [26]. Furthermore, similar oscillatory behaviors originated from different external influences and not intended for LZS interferometry,

have been reported in other types of systems. For example, using self assembled quantum dots [27] under a strain field, quantum dots in micro cavities under terahertz laser excitation [28] or coupled semiconductor nano rings with varying inter-ring distance [29].

In this paper we present practical methods to manipulate electron localization and to cause energy levels' oscillation in quantum confined systems using controlled deformations that can, in principle, be applied at room temperature. These methods can be used to realized LZS interferometry where the oscillation is caused by various means. By deforming the quantum system, the system potential energy is slightly altered and hence the states and their energies are changed accordingly. The practical application of these ideas depends on the magnitude of the level oscillation and displacement of the localization centers, and how these are coupled to the externally controlled deformations. We found that the control of the state localization is easily achievable with deformations. The control of the energy levels requires careful engineering addressing the binding strength of the electron to particular sites that can be obtained using, for example, quantum dots. The assumed controlled deformations are applied either by voltage biasing or pressure across 2D layered systems such as graded semiconductor quantum wells [30–32] or stacks of 2D hybrid perovskites [9, 33]. Thus, the problem becomes a piece-wise constant potential and hence it has an analytical solution [34, 35] where the eigenfunctions, which are exponential and trigonometric functions with continuous logarithmic derivative, and the eigenenergies are obtained as solutions of transcendental algebraic equations. Also, the problem can be solved numerically using various methods like finite difference (FDM) [36, 37], finite element (FEM) [38, 39], and spectral methods [40–44]. In this work, we use a flexible FDM [37] to calculate the eigen-pairs.

The numerical calculations show that energy level oscillations are achievable and manipulatable in the studied systems by controlled deformations. Furthermore, the obtained oscillations are associated with avoided crossings. Thus, it can be used to realize LZS interferometry using alternative means other than the time-varying field. It is shown also that beside the oscillations, the deformation results in changing the spatial localization of the electrons. This should provide means to manipulate the electrons and hence can be used for other applications of quantum-confined systems. The next section presents three different scenarios of controlled deformations, followed by a final section with our general conclusions.

2. Controlled deformations

In order to explore possible scenarios in which localization/delocalization transitions occur via controlled deformations and how are they linked to energy level oscillations we studied three different confined systems. The first one is a graded quantum well between infinite walls where the deformation is modeled by varying spatially the graded potential. The second studied systems is a symmetric multiple quantum well between infinite walls under the effect of biasing voltage. The third system is a layered 2D hybrid perovskites where the pressure is used to induce deformation. Tuning the properties through pressure has been applied for purely inorganic systems [32, 45]. However, the softer character of organic layers should lead to more pronounced effects in 2D hybrid materials [9, 10]. For the calculations, we use a flexible finite FDM [37] for the calculations as aforementioned and atomic units are assumed throughout the paper.

2.1. Graded quantum well between infinite walls

The system analyzed in this subsection is a square well between two infinite walls separated by a distance L. So, the potential (Figure-1) is simply

$$V(x) = \begin{cases} 0 & \text{if} \quad 0 < x < d \text{ or } d + a < x < L \\ -U & \text{if} \quad d < x < d + a \\ \infty & \text{otherwise} \end{cases} , \tag{1}$$

where L, d, a and U are all positive constants and $d + a < L$. The potential deformation is modeled by varying d, which is the distance between the left infinite wall and the edge of the well. Namely, the deformation represents to displace the position of the potential well with respect to the confining walls. As an example of the effects we show some of the results obtained with $L = 15$, $a = 2$, and $U = 3$. In this case, we obtain two states with energy levels below zero (shown in lower left of Figure-1) that are bounded stated to the small well. The energies above zero as a function of d are shown in the right panel of Figure-1, up to the 20th level. It is clear that these states are oscillating with d and that the amplitude of the oscillations depends not in a monotonic way with the order of the level.

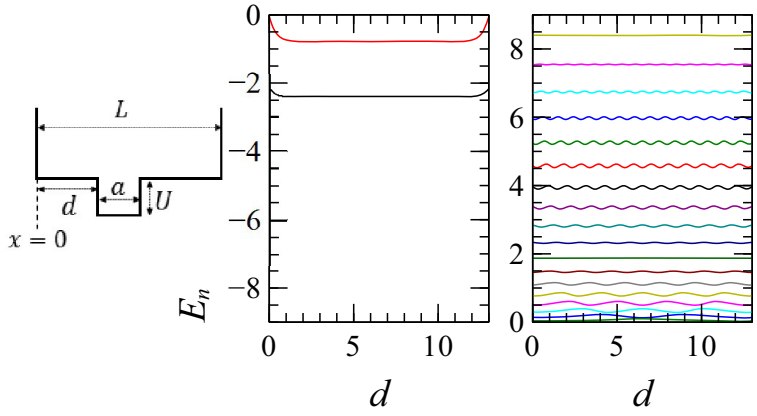

Figure 1. (left) The studied single-well structure. (middle and right panels) Numerical calculation of the first 20 eigenenergies for the example system ($L = 15$, $a = 2$, $U = 3$). The eigenenergies less than zero are shown in the bottom left panel while those greater than zero are shown in the right panel.

In order to have an analytical perspective that could shed light into the different contributions that result on the observed oscillatory behavior, the non degenerate eigenenergies (above zero in the used model) are calculated using perturbation theory (PT). In this case, the unperturbed structure is assumed to be an infinite walls potential and the perturbation is due to the small finite well. So, the Hamiltonian can be rewritten as $H = T + V_0 + V_1$, where

$$V_0(r) = \begin{cases} 0 & \text{if} \quad 0 < x < L \\ \infty & \text{otherwise} \end{cases} \tag{2}$$

and

$$V_1(r) = \begin{cases} -U & \text{if} \quad d < x < d + a \\ 0 & \text{otherwise} \end{cases} \tag{3}$$

The well-known eigenvalues of H_0 $(T + V_0)$ are $E_m^{(0)} = \frac{1}{2}k_m^2 = \frac{1}{2}\left(\frac{m\pi}{L}\right)^2$, where $m = 1, 2, \ldots$, is the sum of peaks and valleys of the corresponding eigenfunctions, which are

$$\psi_m(x) = \sqrt{\frac{2}{L}} \sin(k_m x) \quad . \tag{4}$$

Here, m is used in this subsection as the counter for the states with energies above zero and should not be confused with n that counts all the states. With the exception of this subsection,

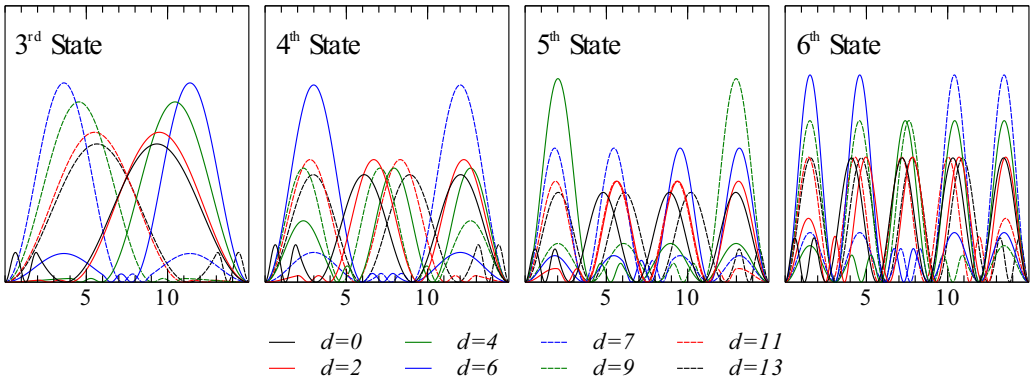

Figure 2. The densities for different states as indicated and selected values if d. As the small well is displaced from left to right there is a concurrent displacement of the density that can be concentrated on either side depending on the state level being observed.

n is used to describe the energy levels throughout this paper. The first order correction to the energies is given by

$$\begin{aligned}\Delta_m^{(1)} &= \langle m\,|V_1|\,m\rangle = -U\int_d^{d+a}\psi_m^2(x)\,dx \\ &= -U\frac{a}{L} + U\frac{1}{m\pi}\sin\left(m\pi\frac{a}{L}\right)\cos\left(m\pi\frac{(2d+a)}{L}\right).\end{aligned} \tag{5}$$

It is clear from the above equation that the corrections are oscillating with d at a frequency of $2m\pi/L$, which matches the oscillations obtained by the numerical calculations especially for higher levels. Eq.-5 also implies that the oscillation amplitude is proportional to U and is sinusoidal with m and a, providing additional means to design and control the oscillations. In particular, the amplitude dependency on m explains the behavior observed on Figure 1 showing stronger oscillations at intermediate values of m.

The localization of the electron, as described by the density $\rho(x) = |\psi(x)|^2$, is also affected by the deformation. In Figure 2 we show the resulted densities for the first four positive eigenenergies, n =3, 4, 5, and 6, for a selection of different d values. There is a clear shifting from one side of the system to the other on the most probable position of the particle as a function of the system state. For example, for the third state, the particle is localized in the right side of the well for $d < (L-a)/2$. The localization is shifted toward the left side for $d > (L-a)/2$. This shifting effect persists up to higher states, although the side chosen by the system depends, among other factor, on the odd/even character of the quantum number.

So far we have shown that energy levels' oscillations (for energies above zero) are directly related to the system's deformation and therefore providing a way to externally control the particular values of the energy spectrum of a system. As aforementioned in the introduction section, many similar oscillations, due to other causes, were reported and in many of them the oscillations are associated with crossing avoidance. The oscillations observed in this example are also associated with density swapping between states. In Figure 3, the energies and densities of the third and forth eigenstates are shown. In the left panel, it is clear that there is a crossing avoidance at $d = 6.5$. This is associated with a density swapping where for $d = 6$, the third state is localized in the left of the well while the fourth state is localized in the right. This swapping happens in the reverse order for $d = 7$.

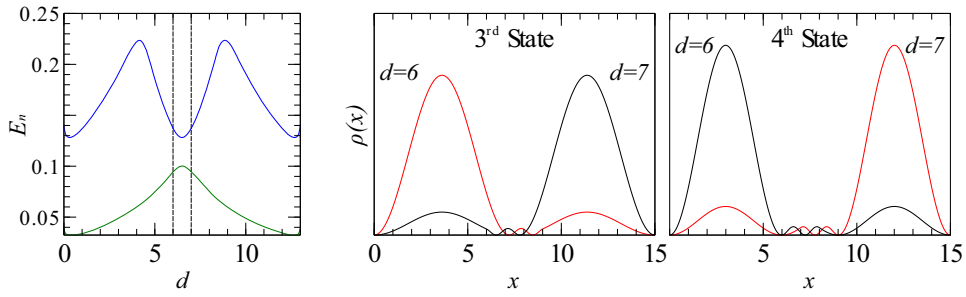

Figure 3. (color online) (left) The energies for the third and forth eignestates vs. d. (middle) The density for the third eigenstate for $d = 6$ and $d = 7$. (right) The density for the firth eigenstate for $d = 6$ and $d = 7$.

2.2. A symmetric multiple quantum well between infinite walls deformed by biasing

In this subsection and the next we consider two examples that could be practically achieved with currently known materials and technologies, allowing the experimental exploration of controlled energy level oscillations and the associated localization/delocalization of the particles. In this case, we start with a symmetric double-well system confined between two infinite walls. Then, a biasing voltage is applied to deform the original system into a tilted one. The unbiased potential, represented in the sketch of Figure 4, is mathematically described by the following potential:

$$V(x) = \begin{cases} 0 & \text{if} \quad |x| < d \text{ or } d + a \leq |x| < L \\ -U & \text{if} \quad d < |x| < d + a \\ \infty & \text{otherwise} \end{cases}, \tag{6}$$

where L, d, a and U are positive constants and $d + a < L$. Equivalent systems can be made although with finite potential walls. For example, using semiconductor multiple quantum wells [46, 47] or a double quantum dot system [48, 49] can be used to realize a device having the qualitative features of Eq. (6). Having this examples in mind, the parameters used in this analysis are within the ranges of practical values. We chose $L = 200$, $a = 40$ and $U = 0.02$ that represent 10 nm, 2 nm and 0.54 eV, respectively. By applying a biasing voltage V_b, the potential is tilted by an additional term of $-V_b\, x$ providing the externally controlled deformation. In our example, the voltage is varied between -0.15 and 0.15 mV. The resulting energies are shown in Figure 4 as a function of V_b, where it can be seen the emergence of an oscillating pattern having similar characteristics to the example of the previous section. For example, the amplitude of the oscillation is a function of the energy level, as it was found by the PT analysis presented above.

Analogously to the case of Subsection A, in this example the energy oscillation has an associated crossing avoidance and localization transition. In Figure 5 we show the energies and densities corresponding to the 11^{th} and 12^{th} eigenstates. In the left panel, it is clear that there is a crossing avoidance around $V_b = 0$ mV. The concurrent density swapping happens upon a very small change in the biasing: for $V_b = -0.01$ mV, the 11^{th} state is localized in the left of the well while the 12^{th} state is localized in the right. The picture is completely reversed for $V_b = 0.01$ mV.

2.3. A layered 2D hybrid perovskites deformed by applying pressure

The second possible practical deformation method that we consider relies on the application of an external pressure. To realize this system we propose a layered 2D hybrid perovskites. These structures are composed of alternating layers of hybrid 2D framework of octahedra inorganic and organic cations providing the wells. Moreover, the system could be intercalated between

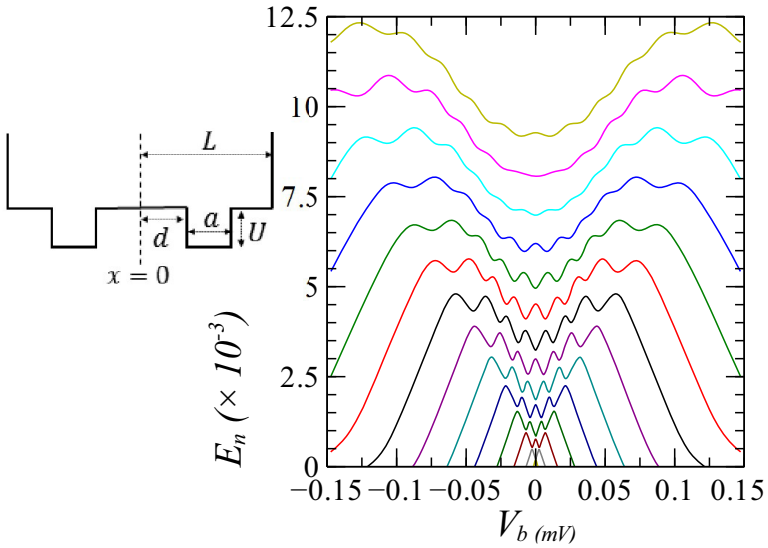

Figure 4. The sketch shows the double-well symmetric structure. The left figure displays the energy levels as a function of the biasing voltage V_b and the induced oscillations. The different colors represent the different energy levels.

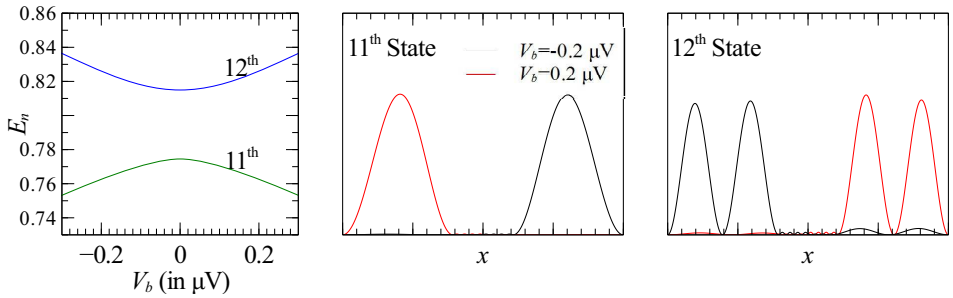

Figure 5. (left) The energies for the 11^{th} and 12^{th} eignestates vs. V_b. (middle) The density for the 11^{th} eigenstate for $V_b = -0.2$ μV and $V_b = 0.2$ μV. (right) The density for the 12^{th} eigenstate for $V_b = -0.2$ μV and $V_b = 0.2$ μV.

softer polymeric layers allowing large deformations and increasing the degree of external control by the application of moderate pressure as compared with purely inorganic crystals [50–52]. These materials can be analyzed as superlattices, as shown by Even et al. [9] and the references therein.

The most studied 2D hybrid materials are $[RNH_3]_2(CH_3NH_3)_{m-1}Pb_mI_{3m+1}$, with R representing an organic group. In these materials, Pb_mI_{3m+1} forms the octahedra that include the (CH_3NH_3) cations forming the wells. On the other hand, $[RNH_3]_2$ constitutes the barriers and by changing the organic group (R), the equilibrium separation between the wells can be tailored [9]. The depth of the well is estimated to be $U_1 = 0.9$ eV [53]. As for the well width, it depends on the number of the octahedra layers. For m =1, 2, 3, and 4, the thicknesses a are 0.65, 1.25, 1.85, and 2.5 nm respectively [53].

In this subsection, we study the effect of the pressure on the energy levels on the $[RNH_3]_2(CH_3NH_3)_{m-1}Pb_mI_{3m+1}$ quantum wells with 1.25 nm barrier. A finite number of wells

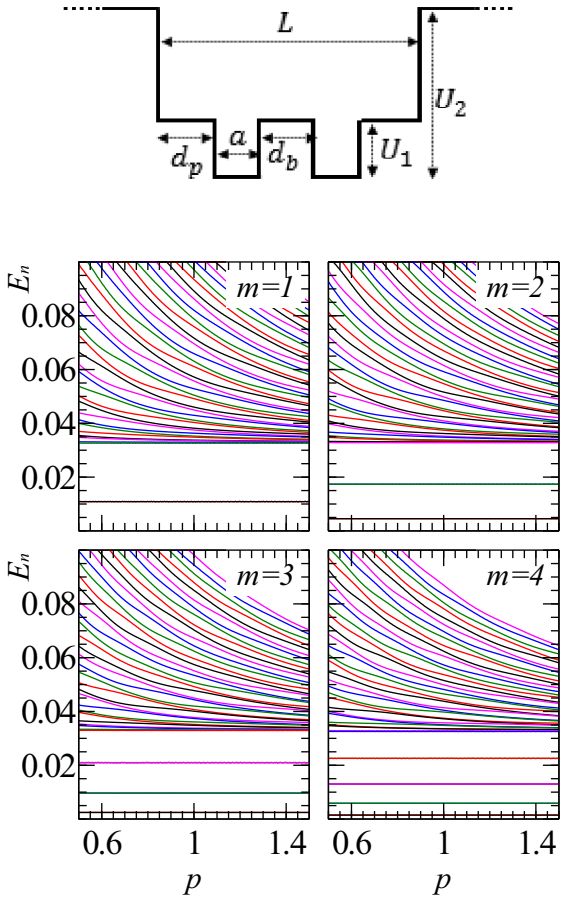

Figure 6. (top) Model potential to represent 2D layer perovskites confined between insulating walls, in this case for two layers creating two confining wells. The deformation affects the external confining layers of width d_p. (bottom) Numerical calculation of the first 40 eigenenergies for a two wells system with m =1, 2, 3, and 4 as a function of the deformation factor.

will be used where the whole system is then placed between two insulators with a barrier height of $U_2 = 2.7$ eV, as described in Figure 6 for the case of two wells [9]. In our approximation, the external pressure only affects the confining external layers by changing their thickness by a factor p. The eigenvalues show the avoidance crossing characteristics as in the previous cases, although now as a function of the deformation parameter p. This is explicitly displayed in Figure 7, in which we display two states corpsonding to the case of $m = 3$. As the system is deformed, the 14^{th} energy level has the particle shifting its preferential position from the central region between the wells for $p = 0.6$, to the outermost layers for $p = 1.4$. The energy level immediately above, the situation is exactly the opposite.

3. Conclusion

In this paper, we have analyzed the interplay between the detailed dimensions of a confining potential, energy level oscillations and particle's localization. It was shown that the obtained oscillations are associated with level avoided crossings and that the deformation induces a change in the preferential spatial localization of the electrons. This effect is quite general, as shown by

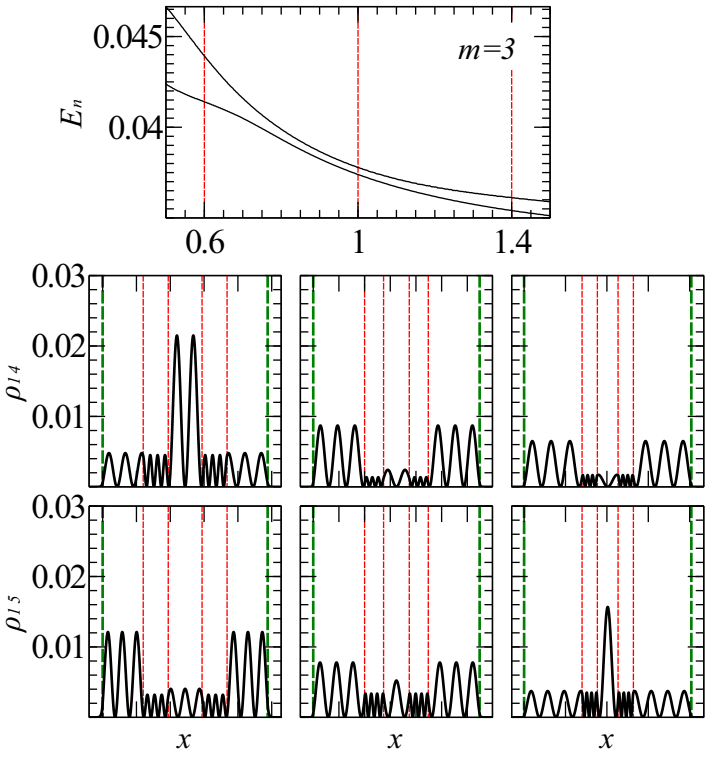

Figure 7. (top) Eigenvalues corresponding the 14^{th} and 15^{th} energy levels for the case of two wells and $m = 3$ as function of the deformation factor (the pressure p). The red vertical dashed lines correspond to the the selected deformations for which the densities are plotted for the two states as function of distance. (bottom) The densities of the two states as function of distance where the dashed green lines are corresponding to the edges of the insulating walls while the dashed red lines are corresponding to the small wells edges.

the the three described examples, and therefore it can be realized in different ways. The external controlling parameter could be an applied voltage or pressure, and other procedures are certainly possible. Obtaining a practical way to experimentally control the electron localization would enable the manipulation of charges in quantum confined systems and provide guidelines for the design of devices. The approach that we have used to describe the is based on simple 1D problems, but the consistent presence of this effect on multiple scenarios suggests that this phenomena is general and could be realized in 3D systems at the nanometer scale.

References

[1] Petta J, Johnson A, Taylor J, Laird E, Yacoby A, Lukin M, Marcus C, Hanson M and Gossard A 2005 *Science* **309** 2180–2184
[2] Taylor J, Petta J, Johnson A, Yacoby A, Marcus C and Lukin M 2007 *Physical Review B* **76** 035315
[3] Schoelkopf R and Girvin S 2008 *Nature* **451** 664–669
[4] Vion D, Aassime A, Cottet A, Joyez P, Pothier H, Urbina C, Esteve D and Devoret M H 2002 *Science* **296** 886–889
[5] Astafiev O, Zagoskin A M, Abdumalikov A, Pashkin Y A, Yamamoto T, Inomata K, Nakamura Y and Tsai J 2010 *Science* **327** 840–843
[6] Berns D M, Rudner M S, Valenzuela S O, Berggren K K, Oliver W D, Levitov L S and Orlando T P 2008 *Nature* **455** 51–57

[7] Niemczyk T, Deppe F, Huebl H, Menzel E, Hocke F, Schwarz M, Garcia-Ripoll J, Zueco D, Hümmer T, Solano E *et al.* 2010 *Nature Physics* **6** 772–776
[8] Zecherle M, Ruppert C, Clark E, Abstreiter G, Finley J and Betz M 2010 *Physical Review B* **82** 125314
[9] Even J, Pedesseau L and Katan C 2014 *ChemPhysChem* **15** 3733–3741
[10] Lanty G, Jemli K, Wei Y, Leymarie J, Even J, Lauret J S and Deleporte E 2014 *The Journal of Physical Chemistry Letters* **5** 3958–3963
[11] Serra P, Carignano M A, Alharbi F H and Kais S 2013 *Europhysics Letters* **104** 16004
[12] Oliver W D, Yu Y, Lee J C, Berggren K K, Levitov L S and Orlando T P 2005 *Science* **310** 1653–1657
[13] Sillanpää M, Lehtinen T, Paila A, Makhlin Y and Hakonen P 2006 *Physical review letters* **96** 187002
[14] Hanson R and Awschalom D D 2008 *Nature* **453** 1043–1049
[15] Vandersypen L M and Chuang I L 2005 *Reviews of modern physics* **76** 1037
[16] Criger B, Passante G, Park D and Laflamme R 2012 *Philosophical Transactions of the Royal Society A: Mathematical, Physical and Engineering Sciences* **370** 4620–4635
[17] Oh S, Huang Z, Peskin U and Kais S 2008 *Physical Review A* **78** 062106
[18] Schirmer S G, Pullen I C and Solomon A I 2005 *Journal of Optics B: Quantum and Semiclassical Optics* **7** S293
[19] Ferrón A, Serra P and Osenda O 2013 *Journal of Applied Physics* **113** 134304
[20] Awschalom D D, Bassett L C, Dzurak A S, Hu E L and Petta J R 2013 *Science* **339** 1174–1179
[21] Shevchenko S, Ashhab S and Nori F 2010 *Physics Reports* **492** 1–30
[22] Yao N Y, Jiang L, Gorshkov A V, Maurer P C, Giedke G, Cirac J I and Lukin M D 2012 *Nature Communications* **3** 800
[23] Zhang J, Yung M H, Laflamme R, Aspuru-Guzik A and Baugh J 2012 *Nature Communications* **3** 880
[24] Zhao Y J, Fang X M, Zhou F and Song K H 2012 *Physical Review A* **86** 052325
[25] Shevchenko S, Ashhab S and Nori F 2012 *Physical Review B* **85** 094502
[26] Zhang J N, Sun C P, Yi S and Nori F 2011 *Physical Review A* **83** 033614
[27] Sheng W and Leburton J P 2002 *Physical review letters* **88** 167401
[28] Sherwin M S, Imamoglu A and Montroy T 1999 *Physical Review A* **60** 3508
[29] Chwiej T and Szafran B 2008 *Physical Review B* **78** 245306
[30] Lenchyshyn L, Liu H, Buchanan M and Wasilewski Z 1996 *Journal of applied physics* **79** 8091–8097
[31] Högele A, Seidl S, Kroner M, Karrai K, Warburton R J, Gerardot B D and Petroff P M 2004 *Physical review letters* **93** 217401
[32] Bardyszewski W and Łepkowski S 2012 *Physical Review B* **85** 035318
[33] Mitzi D B, Chondroudis K and Kagan C R 2001 *IBM journal of research and development* **45** 29–45
[34] Flügge S 1994 *Practical quantum mechanics* (Springer Verlag)
[35] Serra P and Kais S 2012 *Journal of Physics B: Atomic, Molecular and Optical Physics* **45** 235003
[36] Harrison P 2000 *Quantum Wells, Wires and Dots: Theoretical and Computational Physics* 1st ed (Chichester: John Wiley & Sons)
[37] Alharbi F 2008 *Optical and quantum electronics* **40** 551–559
[38] Nakamura K, Shimizu A, Koshiba M and Hayata K 1989 *Quantum Electronics, IEEE Journal of* **25** 889–895
[39] Le K Q 2009 *Microwave and Optical Technology Letters* **51** 1–5
[40] Alharbi F 2010 *Physics Letters A* **374** 2501–2505
[41] Alharbi F 2009 *Optical and quantum electronics* **41** 751–760
[42] Alharbi F and Scott J C 2009 *Optical and quantum electronics* **41** 583–597
[43] Alharbi F H and Kais S 2013 *Physical Review E* **87** 043308
[44] Lin W, Kovvali N and Carin L 2006 *Computer physics communications* **175** 78–85
[45] Meyer R, Dahl M, Schaack G, Waag A and Boehler R 1995 *Solid state communications* **96** 271–278
[46] Lumb M P, Yakes M K, González M, Vurgaftman I, Bailey C G, Hoheisel R and Walters R J 2012 *Applied Physics Letters* **100** 213907
[47] Christmann G, Askitopoulos A, Deligeorgis G, Hatzopoulos Z, Tsintzos S I, Savvidis P G and Baumberg J J 2011 *Applied Physics Letters* **98** 081111
[48] Stafford C A and Wingreen N S 1996 *Physical review letters* **76** 1916
[49] Hu X and Sarma S D 2000 *Physical Review A* **61** 062301
[50] Frost J M, Butler K T, Brivio F, Hendon C H, van Schilfgaarde M and Walsh A 2014 *Nano Letters* **14** 2584–2590
[51] Angel R, Zhao J and Ross N 2005 *Physical review letters* **95** 025503
[52] Schaak R E and Mallouk T E 2002 *Chemistry of Materials* **14** 1455–1471
[53] Tanaka K and Kondo T 2003 *Science and Technology of Advanced Materials* **4** 599–604